Available online at www.sciencedirect.com

ScienceDirect

Geochimica et Cosmochimica Acta 198 (2017) 1–16

Geochimica et Cosmochimica Acta

www.elsevier.com/locate/gca

Distribution of Sb, As, Ge, and In between metal and silicate during accretion and core formation in the Earth

K. Righter [a,*], K. Nickodem [b,1], K. Pando [c], L. Danielson [c], A. Boujibar [a], M. Righter [d], T.J. Lapen [d]

[a] Mailcode KT, NASA Johnson Space Center, 2101 NASA Pkwy., Houston, TX 77058, United States
[b] Department of Civil Engineering and Geological Sciences, University of Notre Dame, Notre Dame, IN 46556, United States
[c] Jacobs JETS, NASA Johnson Space Center, 2101 NASA Pkwy., Houston, TX 77058, United States
[d] University of Houston, Dept. of Earth and Atmospheric Sciences, Houston, TX 77204, United States

Received 31 March 2016; accepted in revised form 27 October 2016; available online 12 November 2016

Abstract

A large number of siderophile (iron-loving) elements are also volatile, thus offering constraints on the origin of volatile elements in differentiated bodies such as Earth, Moon, Mars and Vesta. Metal–silicate partitioning data for many of these elements is lacking, making their overall mantle concentrations in these bodies difficult to model and origin difficult to distinguish between core formation and volatile depletion. To address this gap in understanding, we have undertaken systematic studies of four volatile siderophile elements – Sb, As, Ge and In – at variable temperature and variable Si content of metal. Several series were carried out at 1 GPa, and between 1500 and 1900 °C, for both C saturated and C-free conditions. The results show that temperature causes a decrease in the metal/silicate partition coefficient for all four elements. In addition, activity coefficients for each element have been determined and show a very strong dependence on Si content of Fe alloy. Si dissolved in metal significantly decreases the metal/silicate partition coefficients, at both 1600 and 1800 °C. The combination of temperature and Si content of the metal causes reduction of the metal–silicate partition coefficient to values that are close to those required for an origin of mantle As, Sb, Ge, and In concentrations by metal–silicate equilibrium processes. Combining these new results with previous studies on As, Sb, Ge, and In, allowed derivation of predictive expressions for metal/silicate partition coefficients for these elements which can then be applied to Earth. The expressions are applied to two scenarios for continuous accretion of Earth; specifically for constant and increasing fO_2 during accretion. The results indicate that mantle concentrations of As, Sb, Ge, and In can be explained by metal–silicate equilibrium during an accretion scenario. The modeling is not especially sensitive to either scenario, although all element concentrations are explained better by a model with variable fO_2. The specific effect of Si is important and calculations that include only S and C (and no Si) cannot reproduce the mantle As, Sb, Ge, and In concentrations. The final core composition in the variable fO_2 model is 10.2% Si, 2% S, and 1.1% C (or $X_{Si} = 0.18$, $X_S = 0.03$, and $X_C = 0.04$. These results suggest that core formation (involving a Si, S, and C-bearing metallic liquid) and accretion were the most important processes establishing many of Earth's mantle volatile elements (indigenous), while post-core formation addition or re-equilibration (exogenous) was of secondary or minor importance.
Published by Elsevier Ltd.

Keywords: Siderophile; Core formation; Volatiles; Activity coefficient; Metal

1. INTRODUCTION

Siderophile elements comprise nearly 30 different elements, each with a common characteristic of having affinity

* Corresponding author.
E-mail address: kevin.righter-1@nasa.gov (K. Righter).
[1] Now at Dept. Geography, Syracuse University, 144 Eggers Hall, Syracuse, NY 13244-1020, United States.

http://dx.doi.org/10.1016/j.gca.2016.10.045
0016-7037/Published by Elsevier Ltd.

for metallic iron. Therefore, they are commonly depleted in the mantle of a differentiated body due to sequestration in the metallic core. The metal–silicate partition coefficients of these elements depend on temperature, pressure, oxygen fugacity, and metal and silicate composition; their absolute values are largely dependent upon thermodynamic equilibrium between metal and silicate melt (e.g., Righter, 2003; Wade and Wood, 2005; Siebert et al., 2011). As a result, siderophile elements have placed constraints on the conditions of core segregation and differentiation in bodies such as Earth, Earth's Moon, Mars, and the eucrite parent body (likely asteroid 4 Vesta). Among the siderophile elements, there are a subset that are also volatile (Fig. 1; volatile siderophile elements or VSE), and thus can help to constrain the origin of volatile elements in these bodies, particularly the Earth. One hypothesis is that they were added and partitioned into the metallic core during Earth's accretion and core formation (e.g., Righter, 2011a). Other studies argue for a multiple stage origin (e.g., Mann et al., 2009), while some hypothesize that volatiles were added after the core already formed (e.g., Yi et al., 2000; Albarède, 2009; Ballhaus et al., 2013). In the most general sense, there is debate about whether volatiles had an indigenous or exogenous origin, and a better understanding of this volatile acquisition is fundamental to theories for Earth's origin and evolution.

The Earth's core is composed of Fe and some lighter constituents (some combination of S, Si, C, O, and H). The effects of S and C on metal/silicate partitioning of trace siderophile elements are known due to research in the steel industry (e.g., Lupis, 1983; Steelmaking Data Sourcebook, 1988), but an understanding of the effects of Si is not as extensive. Given the recent interest in Si as a light element in Earth's core (e.g., Ziegler et al., 2010), and demonstration that Si can have a significant effect on the magnitude of D(metal/silicate) (Tuff et al., 2011; Righter et al., 2016), it is of great interest to determine the specific effect of Si on the partitioning of siderophile elements between metal and silicate melt. Many of the VSE exhibit well defined depletions in Earth's mantle (Witt-Eickschen et al., 2009; McDonough and Palme, 2014) but their behavior in metal–silicate systems have yet to be studied comprehensively. For example, the partitioning of some VSE is known to be dependent upon the S or C content of metal (e.g., Ge; Jana and Walker, 1997b; Siebert et al., 2011; Wood et al., 2014), and some of these have been studied

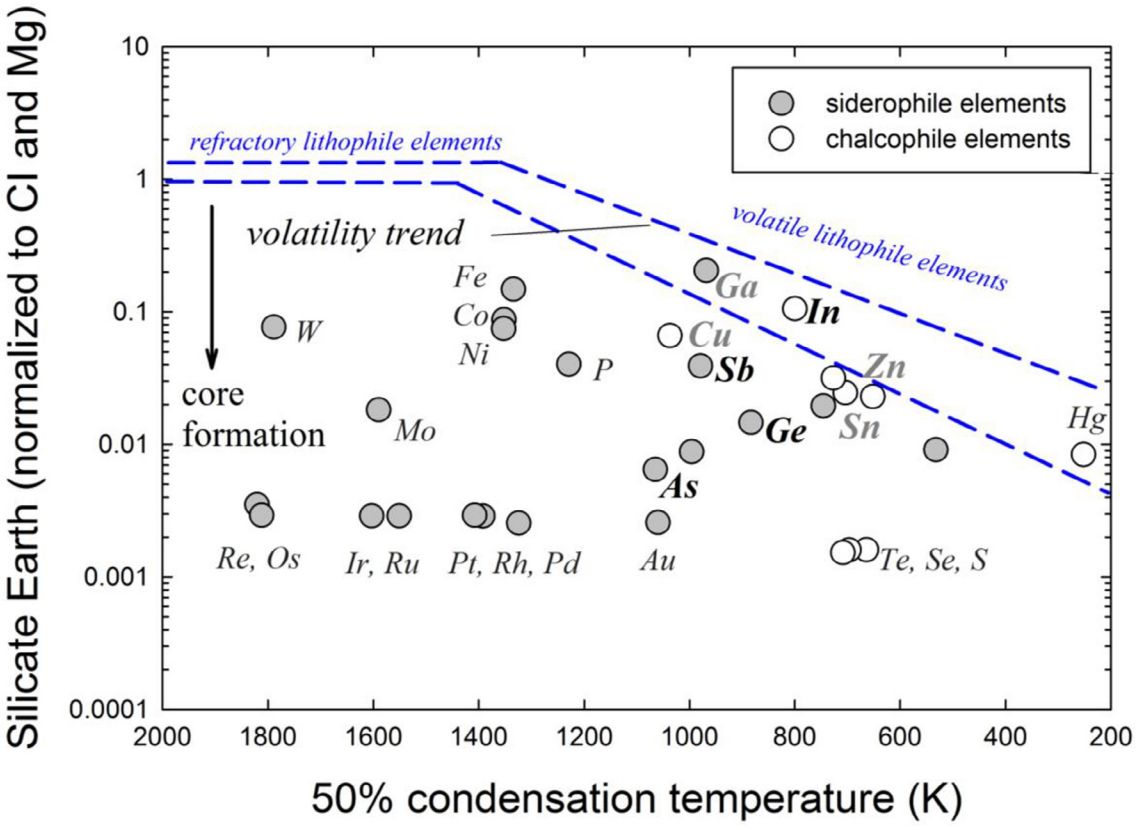

Fig. 1. Concentrations of siderophile elements in the terrestrial primitive upper mantle, relative to CI chondrites, plotted against 50% condensation temperature for the metal (after Palme and O'Neill, 2014). Depletions of volatile siderophile elements are due in part to volatility, as shown by region between dashed lines. Germanium, antimony, and arsenic plot below the volatility trend indicating that a further depletion is likely due to core formation. Condensation temperatures for elements are commonly tabulated in 50% values (taken from Lodders, 2003) which indicate the temperature at which the element falls to 50% of its initial value in the gas (e.g., Wasson, 1985); the abundances of the volatile elements are thought to be a reflection of condensation processes in the early solar nebula. Volatility corrections for Ge, In, Sb, and As are 3, 4, 3 and 3, respectively, based on this figure and the discussions in text for In (see text and Table S4 for more details).

at high temperature, pressure, and variable fO_2 (e.g., In, Zn; Mann et al., 2009), whereas others are only well understood at the reconnaissance level (e.g., Sb, Cd; Righter, 2007, 2009; Ballhaus et al., 2013) or with respect to one or two variables such as temperature or melt composition (e.g., Ge; Righter et al., 2011a). Therefore studies of systematic behavior of the volatile siderophile elements (VSE) are needed in order to improve the quantitative modeling of these elements during core formation and planetary differentiation.

As, In, Ge, and Sb are all volatile siderophile elements (VSE) with well-defined mantle depletions, and for which there exists some understanding of partitioning behavior. But there nonetheless are some critical gaps in understanding, such as the effect of temperature and Si content of the Fe alloy are not well understood. Reported here are the results from 20 experiments examining the partitioning of As, In, Ge, and Sb between silicate and metallic liquid. These experiments will examine the effect of temperature and metal Si composition on these elements in order to gain a greater understanding of their behavior during core-mantle separation in the Earth's early stages. We will use the new data in combination with previous studies to place constraints on how much of the volatile siderophile element depletions are due to core formation vs. volatility.

2. EXPERIMENTAL PROCEDURES

The samples used for the series of experiments were powders composed of 70 wt.% Knippa Basalt, composition described in Lewis et al. (1993), 30 wt.% metal mixture, and varying amounts of Si ranging from 0 to 10 wt.% Si. The metal mixture contained 80.9 wt.% Fe, 8.2 wt.% FeS, 2.4 wt.% Ge, 3.2 wt.% As_2O_3, 2.9 wt.% Sb_2O_3, and 2.4 wt.% In. These were ground into a powder and mechanically mixed. These wt.% concentrations of Ge, As, Sb and In are used because the solubility of Ge, Sb and As is known to be low in silicate melts (low ppm levels for Sb and As; Righter et al., 2009), and therefore enough must be added to achieve measurable amounts in the silicate melt after equilibration. For In, the solubility is high in silicates, but low in metallic liquids, so we have added enough to maintain measurable quantities in the metallic phase. These levels are higher than the levels in the natural Earth, but still lower than levels used in many widely cited and utilized experimental studies on similar siderophile elements such as W (Cottrell et al., 2009), Mo (Walter and Thibault, 1995), and Ni (Kegler et al., 2008). Henrian behaviour was observed by Chabot et al. (2003) for Ge and As (and 10 other trace elements) in metallic liquid–solid systems across this concentration range, and it is assumed here that this is also valid for In and Sb.

The runs were conducted using a piston cylinder apparatus at constant pressure of 1.0 GPa with various times and temperatures. Once at constant pressure, samples were heated to high temperatures to melt and attain equilibrium for durations based on diffusion time across the capsule (e.g., Li and Agee, 2001; Righter et al., 2010), and a time series (see Section 4.2. below). Run durations were 180 min at 1500 °C, 90 min at 1600 °C, 45 min at 1700 °C, and 15 min at 1800 and 1900 °C (Table S1). The temperature was measured using type C thermocouple (W-Re) wires with an accuracy of ±2 °C; temperature variation over the length of the capsule may have been ~10 °C (Musselwhite et al., 2006). Samples were then quenched to a silicate glass (or a matte of quench crystals in the case of most of the MgO capsule experiments) with large metallic spheres (Fig. 2) by turning off the power and keeping constant pressure until the temperatures reached 100 °C.

Four series were performed (Table S1): two series with varying amounts of Si in the metal performed at 1600 °C and 1800 °C in graphite capsules, a third series with varying amounts of Si in the metal performed at 1600 °C and using MgO capsules, and a fourth series with temperature ranging between 1500 °C and 1900 °C. Silicon metal was added to experiments to promote more reduced conditions – Si alloys with the Fe at high temperatures, producing conditions between 4 and 8 log fO_2 units below IW buffer depending on the concentration of Si in metal (see Secion 4.3. below). This approach has also been used by Berthet et al. (2009), Gessmann et al. (1999) and others to produce a reduced environment in high pressure sample assemblies.

3. ANALYTICAL DETAILS

Samples were analyzed for major element composition using a Cameca SX100 for electron microprobe analysis (EMPA) at NASA-JSC. A 1 μm beam was used at 20 kV and 10 nA, and rastered analysis allowed coverage of larger areas (10 μm × 10 μm) for any given point, which provided a larger sampling area for metallic and silicate liquids that had quenched to multi-phase quench textures (see results section). For each sample 15–50 points were analyzed and averaged to obtain a representative analysis of the quenched silicate or metallic liquids. Metal standards were Fe, Ge, InP, Sb, As, Fe_3C, and Si, and silicate standards were natural feldspars (Na and K), glasses (Si, Al, Fe, Mg, and Ca), rhodonite (Mn), rutile (Ti), and apatite (P). In many experiments graphite capsules were utilized and thus the metals contained carbon; carbon was analyzed using the standards and approach of Dasgupta et al. (2013). Carbon contents ranged from 1.7 to 6.0 wt.%, and all elements were re-calculated using the measured C contents in the matrix corrections. Analytical uncertainties are 2% (of the amount present) for Ti, Fe, Mn, Ca, K, and 5% (of the amount present) for Si, Al, Mg, Na, P in glasses and C, As, Sb, Ge and In in metals.

For most samples the In, As, Sb, and Ge content of the glass was lower than the detection limits of the EMPA; therefore, the samples were analyzed for trace element composition using laser ablation inductively coupled plasma mass spectrometry (LA-ICP-MS) at Rice University (Agrinier and Lee, 2007; Righter et al., 2010) and at the University of Houston (Tables S1 and S2). Prior to laser analysis, the run products were characterized by BSE imaging and major element abundances were determined by electron probe microanalysis (EPMA) at the NASA Johnson Space Center.

The Rice University LA-ICP-MS system (ThermoFinnigan Element 2 magnetic sector ICP-MS coupled with a

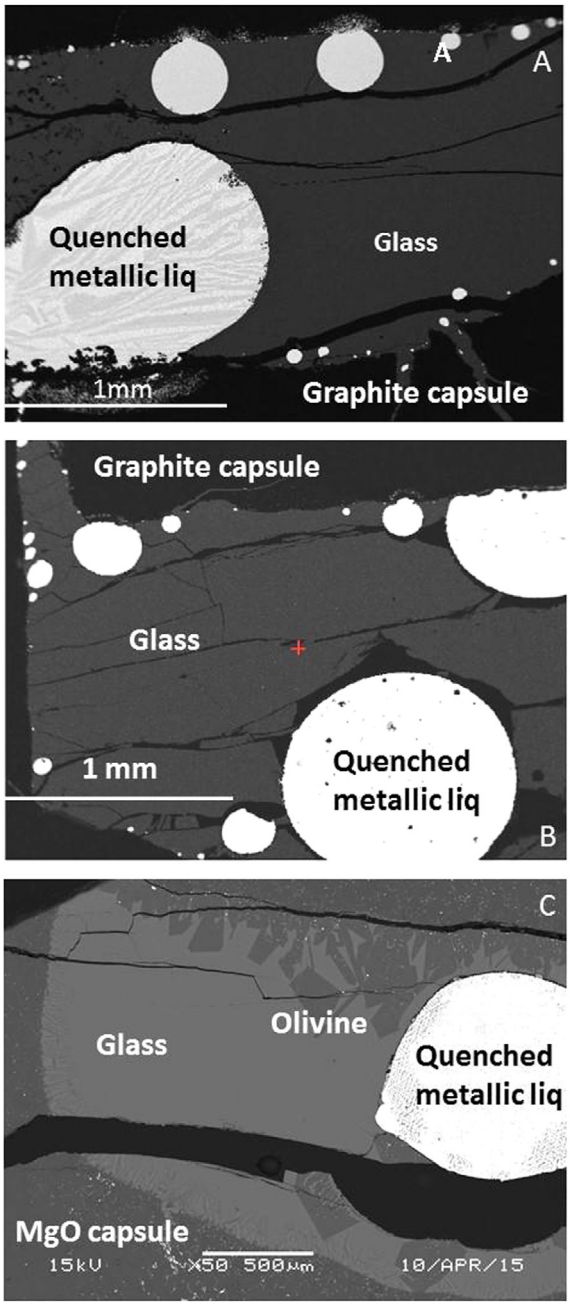

Fig. 2. (A) Back scattered electron (BSE) image of experiment KAN160-60 (graphite capsule) run for 60 min at 1600 °C °C, with Si-free metal and relative fO_2 of $\Delta IW = -1.40$; (B) BSE image of experiment KAN186D (graphite capsule) run for 15 min at 1800 °C, 6% Si added, and relative fO_2 of $\Delta IW = -4.42$. The samples resulted in quenched metallic liquid (white) surrounded by silicate glass (gray) which is encased in the graphite capsule (black). Smaller metallic droplets have slightly different appearance (and brightness) because they quenched to a finer grain size compared to the larger droplets that cooled slower and formed coarser quench crystals. The overall composition of the small and large droplets, however, is the same. (C) BSE image of experiment KAN 164 m (MgO capsule) run for 90 min at 1600 °C, with 4% Si added to the metal and relative fO_2 of $\Delta IW = -6.01$.

New-Wave 213 nm laser) was used to analyze all glasses from the experiments run in graphite capsules. For these, the laser was set at 10 Hz pulse frequency and an energy density of 10 mJ/cm^2. Spot size varied from 50 to 200 µm (30–40 µm depth), depending on the size of the sample, but most spots were 200 µm to maximize the area and volume being measured. Measurements consisted of about 10 analyses of gas flow background followed by 40–50 measurements of the ablation signal. Gas background was averaged and then subtracted from ablation signal. Background-corrected signals were converted to concentrations using a combination of internal and external standards. Standards used were NIST-610, NIST-612, BCR-2 g, BHVO-2 g, and BIR-1 g. Analyses of the isotopes ^{75}As, ^{115}In, ^{73}Ge, ^{74}Ge, and ^{121}Sb were performed in low resolution (LR) mode and normalized to ^{43}Ca. Given the time resolved nature of the analysis, the effects of small interfering metallic particles on the glass analyses could be monitored and filtered out during the subsequent data processing (Fig. S1). Analytical uncertainties are 10% (of the amount present) for As, Sb, Ge, and In, and the resulting concentrations and error in the partition coefficients (15% which reflects the combination of EMPA and LA-ICP-MS error) are shown in Table S1, and comparison of literature and secondary standard values in Table S2; values presented are the average of three different points on each sample.

Analyses of the MgO series experiments (KAN-160m, -164m, -166m, -168m and -1610m) were performed at University of Houston using a Photon Machines Analyte. 193 ArF laser ablation system coupled to a Varian 810-MS ICP-MS. During LA-ICP-MS, we measured ^{25}Mg, ^{29}Si, ^{43}Ca, ^{51}V, ^{52}Cr, ^{55}Mn, ^{63}Cu, ^{66}Zn, ^{69}Ga, ^{72}Ge, ^{75}As, ^{115}In, ^{113}In, ^{118}Sn, and ^{121}Sb. For the analysis of these experiments, we used a round 49.3 µm diameter laser spot at the sample surface, a repetition rate of 8 Hz, and a laser power setting of 2.99 J/cm^2. The carrier gas used to carry ablated material to the detector was He at a flow rate of 500 ml/min. For each analyzed point, we measured a 20 s gas blank prior to sample ablation, followed by ~30 s ablation on the sample. All trace element data were corrected for laser and ICPMS elemental fractionation with NIST 612, and ^{43}Ca as an internal standard. Data were reduced using the Glitter software (van Achterbergh et al., 1999). Values presented in Table S1 are the average of three different points on each sample. Two experimental glasses – 180F and 190F – were analyzed using both the Rice and UH LA-ICP-MS instruments and give results that are identical within the error of the measurements (Table S2).

4. RESULTS

4.1. Phase equilibria

All experimental products consisted of large silicate melt portions surrounding liquid metallic iron alloy. Silicate melts in the graphite capsule experiments quenched to a glass, whereas those in the MgO capsule experiments quenched to glass and crystals due to the higher MgO content of these liquids. Several of the MgO capsule

experiments contain coarse olivine grains near the top of the capsule – these were avoided during analysis of the silicate because they grew at equilibrium conditions and were not part of the melts. The metallic portions do not quench to a single phase, but rather quench to a texture of Fe and Fe−C−Si alloys (there is a small amount of S in some) (Fig. 2). The trace elements Ge, Sb, As, and In dissolved completely into the Fe metallic liquid; there is no evidence for saturation with pure As or Sb phases, for example. Carbon contents of the Si-free series metallic liquids range from 4.2 to 5.3 wt.% C. For the Si-bearing metallic liquids, C contents decrease to as low as 1.7 wt.% C in the most Si-rich metallic liquids. This inversely correlated variation of Si and C is consistent with previous studies in the Fe−Si−C system (e.g., Morard and Katsura, 2010). Some experiments experienced cracked capsules, and mobility of BaO from the $BaCO_3$ pressure medium into the sample capsule was a problem. In these cases, we re-ran samples so that Ba contamination did not interfere with the desired partition coefficient measurements.

4.2. Equilibrium

In order to demonstrate the necessary experiment duration to approach equilibrium, a time series was carried out at 30, 60, 90, and 120 min (Table S1; experiments 160–30, 160–60, 160B, and 160–120, respectively). These experiments yield nearly identical partition coefficients after 60 min at 1600 °C, consistent with an approach to equilibrium conditions (Fig. S2), so all experiments at 1600 °C had run durations of 90 min to ensure an approach to equilibrium. Slight differences from run to run are caused by slightly different oxygen fugacities as well as variation in metallic liquid composition (C content; Table S1). In addition to the time series, we have analyzed transects across metallic beads and found them to be homogeneous from edge to core to edge (Fig. S3). Finally, the experiments reported here are longer than experiments for which time series have been done for slow diffusing elements such as W^{4+} and P^{5+}, as well as Ga^{3+} and Sn^{4+} (Righter et al., 1997; Righter and Drake, 1999, 2000).

4.3. Oxygen fugacity

As mentioned above, Si metal was added to experiments to promote more reduced conditions – Si alloys with Fe at high temperatures, and an increase in Si content will cause a decrease in fO_2. Oxygen fugacity was calculated relative to the iron-wüstite (IW) oxygen buffer using the expression $\Delta IW = -2\log [X_{Fe}/X_{FeO}]$. The ΔIW values ranged from ~−1.3 to −1.37 for Si free runs compared to Si bearing runs which produced ΔIW values from −4.9 to −7.9 (Table S1). If activities of Fe and FeO are considered, the equation becomes $\Delta IW = -2\log [a_{Fe}/a_{FeO}]$. In this case a_{Fe} can be calculated using the MetalAct epsilon parameter model for metallic liquids of Wade and Wood (2005), and a_{FeO} can be calculated in silicate melt using the results of Holzheid et al. (1997). ΔIW values calculated using activities instead of mole fractions are slightly higher, ranging from IW −0.66 to −7.10 (Table S1). Because most studies utilize the first approach, we include those in the tables and figures, but it is important to note the difference in these approaches given the non-ideality in the Fe–Si–C system; activities are used in later calculations in Section 4.6. The range of ΔIW values for these experiments falls in the range typically considered during Earth's core formation.

4.4. Partition coefficients

Partitioning behavior of As, Sb, Ge, and In can be calculated in two ways. The standard approach uses the distribution coefficient which is simply the weight ratio of the element in the metal and the silicate melt, or D(i) metal/silicate = wt fraction i in metal/wt fraction i in silicate melt. Although this approach is simple and commonly applied, D(i) for these elements can be sensitive to small changes in fO_2 and can make comparison of runs difficult. In addition, plots of log D vs. logfO_2 can yield misleading information about elemental valence due to variations of siderophile element activity with metal composition (see Figs. S4 and S5). However, by using an exchange reaction of a siderophile element with iron and iron oxide, the effect of small changes in fO_2 can be minimized, thus experimental runs can be more directly compared (see for example, O'Neill 1992 or Tuff et al., 2011). For example, equilibrium with siderophile element M of valence n can be written as follows:

$$MO_{n/2}^{silicate} + (n/2)Fe^{metal} = M^{metal} + (n/2)FeO^{silicate} \quad (1)$$

The exchange coefficient, or K_d, can be calculated for each sample using the equation:

$$K_d = \frac{\left[a_M^{metal}\right]\left[a_{FeO}^{silicate}\right]^{n/2}}{\left[a_{MO(n/2)}^{silicate}\right]\left[a_{Fe}^{metal}\right]^{n/2}} \quad (2)$$

where a_M and $a_{MOn/2}$ = activity of element M in the metal and $MO_{n/2}$ in the silicate respectively. The K_d approach is used in the initial analysis of the results of our study because K_d will be independent of fO_2 if the valence is constant over the range of fO_2 investigated. For these four elements, there are some constraints on the valence at fO_2 conditions relevant to core formation (near IW-2), and there is no evidence that valence may change at more reduced conditions. For example, Germanium is divalent based on the studies of Kegler and Holzheid (2011) and Righter et al. (2011a); we have chosen 2+ rather than 3+ suggested by Siebert et al. (2011) due to the better fO_2 constraints of the former studies. Antimony is Sb^{3+} based on Righter et al. (2009) and Capobianco et al. (1999), who also note that valence assessments need to account for activity changes in the metal. In should be 3+ based on partitioning studies of Suzuki and Akaogi (1995), and the regression analysis carried out below; the lower valence of 1+ used by Mann et al. (2009) may be attributed to assuming metal activity coefficients are constant. Finally, we have chosen trivalent arsenic; even though Siebert et al. (2011) found evidence for As^{5+}, systematic treatment of the data for As does not reveal such a strong fO_2 dependence (or high

valence) for As, and is instead consistent with As^{3+}. Therefore we consider the following equilibria:

$$3FeO + 2In = 3Fe + In_2O_3 \quad (3a)$$

$$FeO + Ge = Fe + GeO \quad (3b)$$

$$3FeO + 2Sb = 3Fe + Sb_2O_3 \quad (3c)$$

$$3FeO + 2As = 3Fe + As_2O_3 \quad (3d)$$

The K_d approach, then, allows evaluation of variable Si content of the metal (if melt composition and temperature and pressure are all constant) on K_d. The K_d approach will also be used to assess the activity coefficient of these elements in Si-bearing Fe metallic liquids in three series, as described below. The partition coefficient approach (D) will be used in the detailed modeling and application to Earth because the D approach allows quantification of fO_2 as well as P, T, and silicate and metallic liquid compositions. Standard error on the partition coefficients is listed in (Tables S1 and S3), and represents the error on metal analysis (5%) combined with error on trace element analysis in silicates (10%).

4.5. Effect of temperature

The results show a general decrease in the D and K_d metal/silicate with increasing temperature for all elements

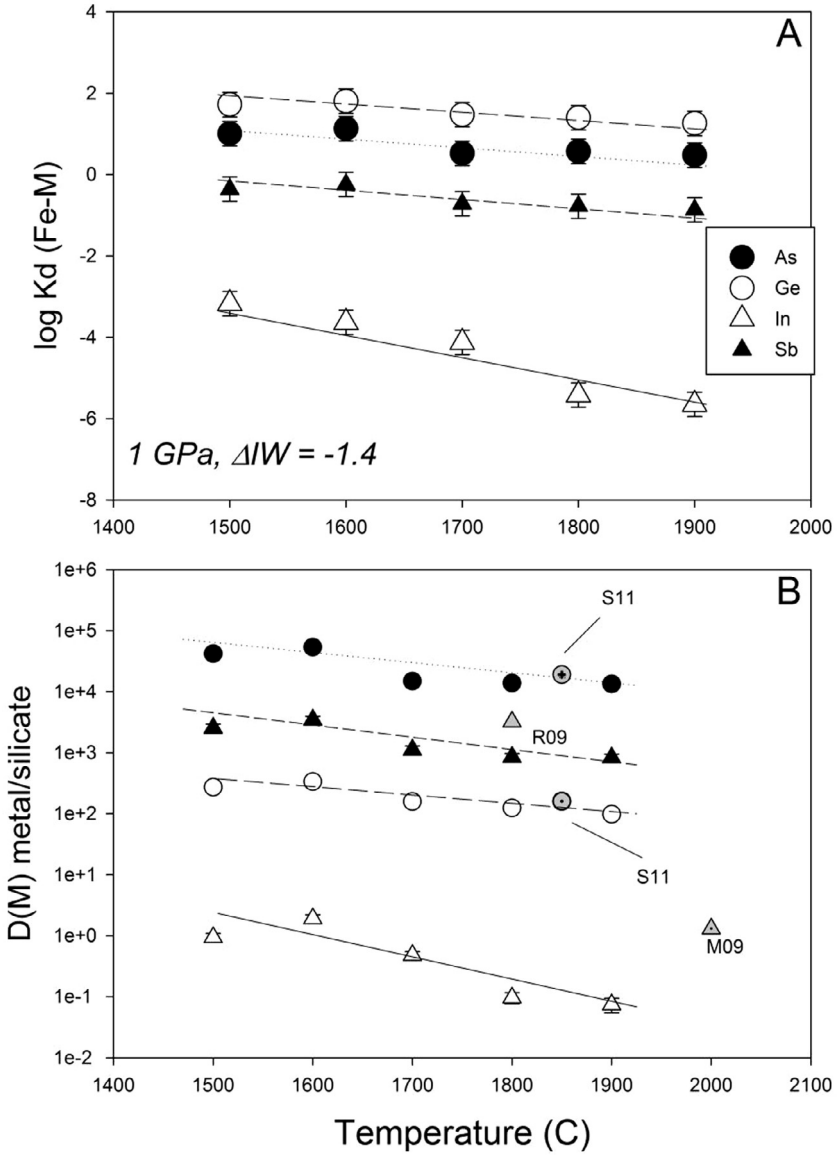

Fig. 3. Log K_d (exchange coefficient) (A) and D(metal/silicate) (B) vs. temperature for the Si-free metal series. Data shows a general decreasing trend with increasing T for all four elements with In showing the strongest effect. All experiments at constant pressure (1 GPa) and nearly constant relative oxygen fugacity ($\Delta IW \sim -1.4$; Table S1). Also shown in panel B for comparison are a few results from previous studies at comparable or similar P, T, and fO_2 conditions. Two experiments from Siebert et al. (2011) show Ge and As results at 1850 °C (S11), one experiment from Righter et al. (2009) showing Sb results at 1800 °C (R09), and one experiment from Mann et al. (2009) showing In results at 2000 °C (M09).

(Fig. 3). Indium shows the strongest dependence on temperature with log K_d values dropping approximately two orders of magnitude over this temperature range (400 °C). The effect of temperature for Ge, Sb and As is smaller, but still approaching 1 order of magnitude. Results for D (As) metal/silicate and D(Ge) metal/silicate at 3 GPa from Siebert et al. (2011) are in excellent agreement with our results, with Siebert et al. (2011) values for log K_d falling along the same line with our results within analytical uncertainty (Fig. 3).

4.6. Effect of Si concentration in the metallic iron

The effect of Si on siderophile element partitioning between metal and silicate can be examined by isolating the effect of Si from the effects of other variables that can change K_d. To circumvent the combined effect of fO_2 and metal Si content, we utilize the Fe exchange coefficient K_d(Fe–M) of Eq. (1), which is independent of oxygen fugacity, and therefore can be used to isolate the effect of Si on M partitioning. Expanding Eq. (2) and following a similar approach to that of Wood et al. (2014) to investigate sulfur,

$$\ln K = \ln \frac{\left[a_M^{metal}\right]\left[a_{FeO}^{silicate}\right]^{n/2}}{\left[a_{MO(n/2)}^{silicate}\right]\left[a_{Fe}^{metal}\right]^{n/2}} = \ln \frac{\left[X_M^{metal}\right]\left[X_{FeO}^{silicate}\right]^{n/2}}{\left[X_{MO(n/2)}^{silicate}\right]\left[X_{Fe}^{metal}\right]^{n/2}} + \ln \frac{\left[\gamma_M^{metal}\right]\left[\gamma_{FeO}^{silicate}\right]^{n/2}}{\left[\gamma_{MO(n/2)}^{silicate}\right]\left[\gamma_{Fe}^{metal}\right]^{n/2}} \quad (4)$$

We set $K_D = \frac{\left[X_M^{metal}\right]\left[X_{FeO}^{silicate}\right]^{n/2}}{\left[X_{MO(n/2)}^{silicate}\right]\left[X_{Fe}^{metal}\right]^{n/2}}$ and assume the ratio of oxide activity coefficients in the silicate, $\frac{\left[\gamma_{FeO}^{silicate}\right]^{n/2}}{\left[\gamma_{MO(n/2)}^{silicate}\right]}$, is fixed, since in this study the silicate melt composition is nearly constant from experiment to experiment. On the other hand, the metal composition varies significantly in Si content and the ratio of activity coefficients in the metal, $\frac{\left[\gamma_M^{metal}\right]}{\left[\gamma_{Fe}^{metal}\right]^{n/2}}$, is dependent upon variations in metal composition. Then Eq. (2) above can be re-arranged to yield $\ln K_D = \text{constant} + n/2 \ln \gamma_{Fe}^{metal} - \ln \gamma_M^{metal}$. When combined with $\ln \gamma_M^{metal} = \ln \gamma_{Fe}^{metal} + \ln \gamma_M^0 - \varepsilon_M^{Si} \ln(1 - X_{Si})$ yields $\ln K_D - (n/2 - 1) \ln \gamma_{Fe}^{metal} = \text{const} - \ln \gamma_M^0 + \varepsilon_M^{Si} \ln(1 - X_{Si})$. Here ε_M^{Si} is an interaction parameter (Lupis, 1983) that can be used to isolate the effect of a solute such as Si (in Fe metallic liquid) on the activity of a trace element such as As, Sb, Ge, and In. The slope of $\ln K_D$ vs. $\ln(1 - X_{Si})$ gives ε_M^{Si} directly for each element at 1600 °C and 1800 °C for the C-saturated experiments and at 1600 °C for the C-free experiments (Figs. 4–6, respectively). Slopes (and associated 1σ error) were determined by linear regression using SigmaStat 12.0 from Systat Software, Inc.

The values of ε_M^{Si} derived here are $\varepsilon_{As}^{Si} = 64.1(39.1)$, $\varepsilon_{Sb}^{Si} = 58.0(27.5)$, $\varepsilon_{Ge}^{Si} = 15.0(2.5)$, $\varepsilon_{In}^{Si} = 15.2(7.7)$ at 1600 °C (carbon saturated), $\varepsilon_{As}^{Si} = 47.3(29.1)$, $\varepsilon_{Sb}^{Si} = 40.5(21.9)$, $\varepsilon_{Ge}^{Si} = 4.6(1.3)$, $\varepsilon_{In}^{Si} = 10.7(1.2)$ at 1800 °C (carbon saturated), and $\varepsilon_{As}^{Si} = 35.9(3.2)$, $\varepsilon_{Sb}^{Si} = 60.9(15.0)$, $\varepsilon_{In}^{Si} = 18.5(5.3)$ at 1600 °C (carbon-free), where the values in parentheses are standard error. The ε_M^{Si} values for Sb and In in the C-free and C-saturated experiments at 1600 °C are identical within error, indicating that dissolved C does not have any effect outside of that attributable to Si. Ge was below detection limits of 1.0 ppm in most of the glasses from the C-free series, so we could not determine ε_{Ge}^{Si} in C-free system, but K_d (Ge–Fe) for the Si- and C-free sample is identical to that in the C-saturated series, suggesting that the values of ε_{Ge}^{Si} in C-free and C-saturated systems are also similar (and consistent with the results of Siebert et al., 2011). Values for ε_{As}^{Si}, on the other hand, are 64.0 in C-saturated series and 30.5 in the C-free series, indicating that both Si and C have a strong effect on As partitioning. The effect of temperature on ε_M^{Si} for all four elements can be assessed. The values of ε_M^{Si} determined for 1800 °C are lower than those for 1600 °C, as predicted.

All of these newly determined values of ε_M^{Si} are large and positive and will have a significant effect on the activity coefficients in Fe metals that contain Si. The magnitude of this effect is important to quantify and is as large as (if not larger than) the effect of S or C on other siderophile elements documented in previous works (e.g., Jana and Walker, 1997b; Righter and Drake, 1999; Wood et al., 2014). For example, Tuff et al. (2011) demonstrated that Mo and W are strongly affected by Si dissolved in Fe metallic liquid with ε_M^{Si} values as high as 18–20. However, values for Sb and As are between 40 and 64, and those for In are comparable to those for Mo and W (Fig. 7). The effect of Si is much larger than that for S for most of these elements (Fig. 7). Using new values of ε_M^{Si} with the activity model of Ma (2001) (see Supplementary Information), the effect of variable Si on $\ln\gamma(M)$ is shown for all four elements in Fig. 8. Ge and In show mild dependence on X_{Si}, as expected from the modest ε_M^{Si} values, whereas As and Sb show much stronger dependence.

5. DISCUSSION

5.1. Concentrations of volatile siderophile elements in the core and mantle of Earth

Terrestrial primitive upper mantle (PUM) values of Ge, In, As, and Sb can be estimated from measurements made on mantle peridotite such as tabulated by McDonough and Sun (1995), Palme and O'Neill (2014) and Witt-Eickschen et al. (2009) (see Table S4). Most of these measurements allow tight constraints on the concentration in the primitive upper mantle (PUM), but there is some disparity of results for As, for example. The estimates provided by Palme and O'Neill (2014) are higher than those of Witt-Eickschen et al. (2009). For this reason both values are considered in the modelling in subsequent sections.

5.2. Regressions

A widely utilized approach for quantifying metal–silicate partitioning of siderophile element considers the equilibrium:

$$M^{metal} + x/4O_2 = MO_{x/2}^{silicate} \quad (5)$$

Considering that $\Delta G = -RT\ln K$, and expanding the free energy term to $\Delta H - T\Delta S + P\Delta V = -RT\ln K$, and the equilibrium constant to $K = (aMO_{x/2})/(aM)(fO_2)^{x/4} = (\gamma MO_{x/2} * xMO_{x/2})/(\gamma M * xM)(fO_2)^{x/4}$. And recombining equals $-\Delta H/RT + \Delta S/R - P\Delta V/RT = \ln[(\gamma MO_{x/2} * xMO_{x/2})/(\gamma M * xM)(fO_2)^{x/4}] = \ln(\gamma MO_{x/2}) - \ln\gamma M + \ln(xMO_{x/2}/xM) - x/4\ln fO_2$.

Rearranging yields:$\ln(xM/xMO_{x/2}) = (\Delta H/R)/T - \Delta S/R + (\Delta V/R)P/T - x/4\ \ln fO_2 + \ln(\gamma MO_{x/2}) - \ln\gamma M$, and substituting $D(M) = xM^{metal}/xMO_{x/2}^{silicate}$, the expression becomes:

$$\ln D(M) = a\ln fO_2 + b/T + cP/T + \ln\left[\gamma_{MO(n/2)}^{silicate}\right] - \ln\left[\gamma_M^{metal}\right] + e \quad (6)$$

Using this approach, and incorporating silicate liquid compositional term nbo/t (ratio of non-bridging oxygens to tetrahedrally coordinated cations; Mysen, 1991; Mills, 1993) as a proxy for the activity coefficient of species M in silicate melt, $\ln(\gamma MO_{x/2})$, (where M = As, Sb, Ge, or In), Eq. (6) becomes:

$$\ln D(M) = a\ln fO_2 + b/T + cP/T + d(nbo/t) - \ln\left[\gamma_M^{metal}\right] + e \quad (7)$$

$$\ln D'(M) = \ln D(M) + \ln\left[\gamma_M^{metal}\right] = a\ln fO_2 + b/T + cP/T + d(nbo/t) + e \quad (8)$$

Constants a through e can be derived by multiple linear regression of existing experimental data. fO_2 is calculated using the IW buffer of Campbell et al. (2009) together with the activity of Fe using the activity model of Ma (2001) and activity of FeO in silicate melt taken from Holzheid et al. (1997).

The $\gamma(M)_{met}$ values are calculated using the activity model of Ma (2001) using epsilon values derived in this study, together with those in Wade and Wood (2005), Wade et al. (2012), Wood et al. (2014), and the Steelmaking Data Sourcebook (1988) (See full expression in Supplementary Information). Values of $\ln\gamma_0$, were −3.91 (Ge), −4.72 (As), −1.0996 (Sb), and 3.28 (In), and temperature dependence is calculated using the Wagner formalism (Wade and Wood, 2005). The activities of metallic species derived from the epsilon parameter approach has

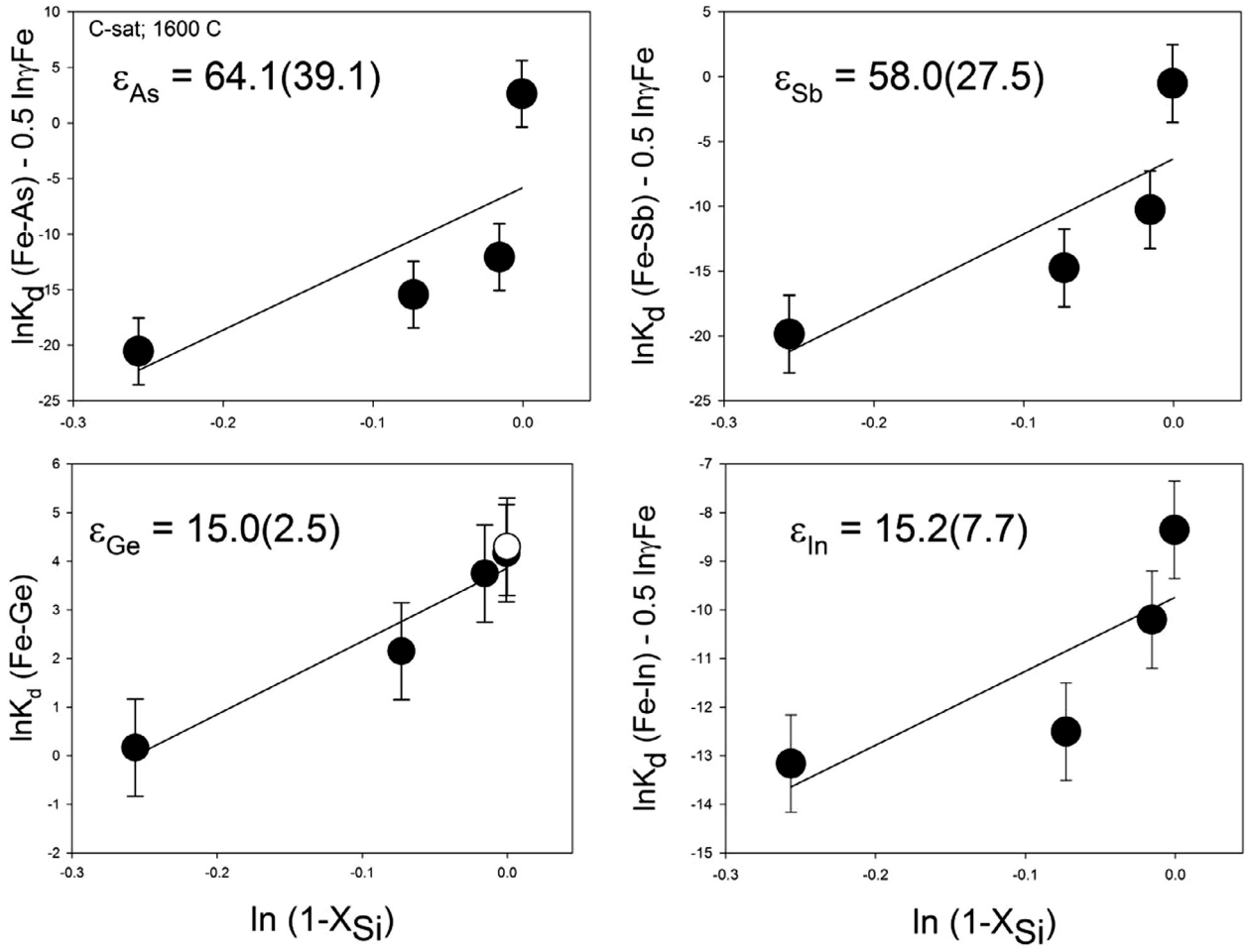

Fig. 4. $\ln K_d$(Fe–M)–(n/2–1) $\ln\gamma_{Fe}^{metal}$ vs. $\ln(1 - X_{Si})$ for As, Sb, Ge, and In at 1600 °C in C-saturated experiments (graphite capsules). Solid lines are a linear fit to the data and the slope of each line is the ε_M^{Si} with associated error. The plot for Ge also includes a point from the C-free series showing that there is no detectable difference between C-saturated and C-free $\ln K_d$ at $X_{Si} = 0$. This suggests C-free and C-saturated conditions affect Ge the same.

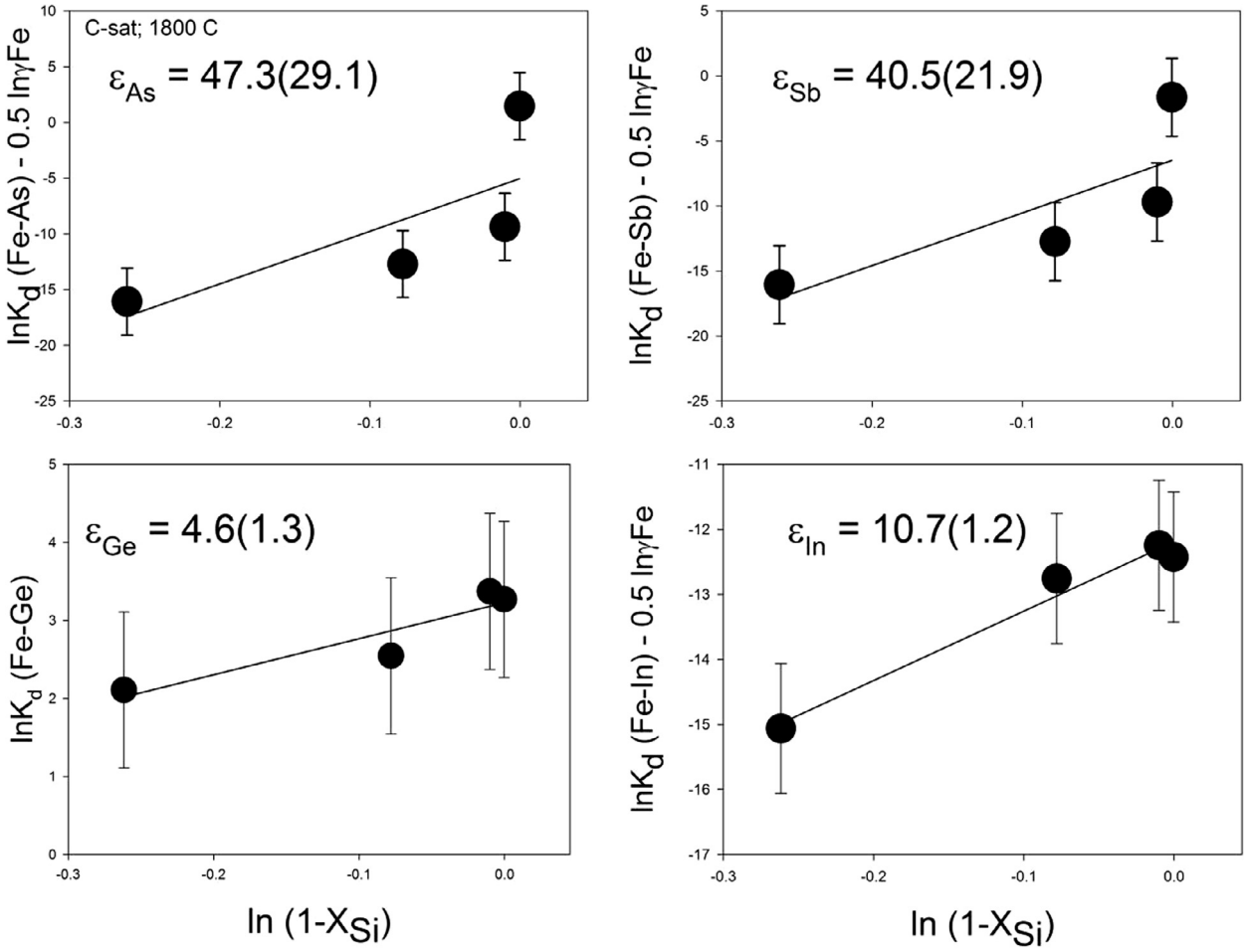

Fig. 5. Ln K_d(Fe–M)–(n/2–1) ln γ_{Fe}^{metal} vs. ln(1 − X_{Si}) for As, Sb, Ge, and In at 1800 °C in C-saturated experiments (graphite capsules). Solid lines are a linear fit to the data and the slope of each line is the ε_M^{Si} with associated error.

also been widely applied in recent studies (e.g., Wade and Wood, 2005; Cottrell et al., 2010; Blanchard et al., 2015).

Partitioning studies available for Ge, In, Sb, and As encompass a wide range of pressure, temperature, oxygen fugacity, and silicate and metallic melt compositions (Table S5). For In, the studies of Mann et al. (2009) and Wang et al. (2016) cover pressure between 2 and 24 GPa, and 1740 to 2600 °C, the study of Ballhaus et al. (2013) includes ultramafic silicate melts, and the studies of Mann et al. (2009), Wang et al. (2016), and this work cover the effects of variable metallic S, C, and Si content. For Ge, the studies of Walker et al. (1993), Hillgren et al. (1996), Jana and Walker (1997a,b) and Siebert et al. (2011) cover the pressure range of 1–18 GPa and 1500-2800 °C. The studies of Jana and Walker (1997b), Walker et al. (1993) include the effect of sulfur dissolved in metallic liquid, Righter et al. (2011a) and Siebert et al. (2011) include the effect of C dissolved in metallic Fe liquid, and this study includes the effect of dissolved Si in metallic liquid. For As, there are two studies but together they include pressure from 0.5 to 18 GPa, and 1500 to 2600 °C, a wide range of fO_2 and silicate melt composition, and incorporate the effects of S, C, and Si in the metallic liquids. For Sb, much data is available, but unfortunately only one datum at pressure >1 GPa, so modelling D(Sb) is currently limited by these data. Nonetheless for Sb the pressure coverage is from 1 to 15 GPa, 1260 to 2180 °C, and includes S, C, and Si bearing Fe metallic liquids across a wide range of silicate melt and fO_2. Data from these studies were regressed against Eq. (8), and traditional statistical tests such as R^2 (coefficient of determination), 2σ error, t values, P values, and F statistics are used to evaluate and ensure the quality of the regressions and the significance of each term (a through e).

These regressions allow separation of the effects of specific variables on the magnitude of the partition coefficient. For example, as pressure and temperature increase along an adiabatic gradient, D(Ge) increases, whereas D(In) metal/silicate and D(As) metal/silicate decreases. These changes are in agreement with individual studies that have been carried out on these elements (Mann et al., 2009; Siebert et al., 2011; Righter et al., 2011a). Because the sensitivity of a partition coefficient on oxygen fugacity depends on its valence, we can examine the coefficients for ln fO_2; these values are consistent with In, As, and Sb as 3+, and Ge as 2+. Finally, the effects of silicate melt composition

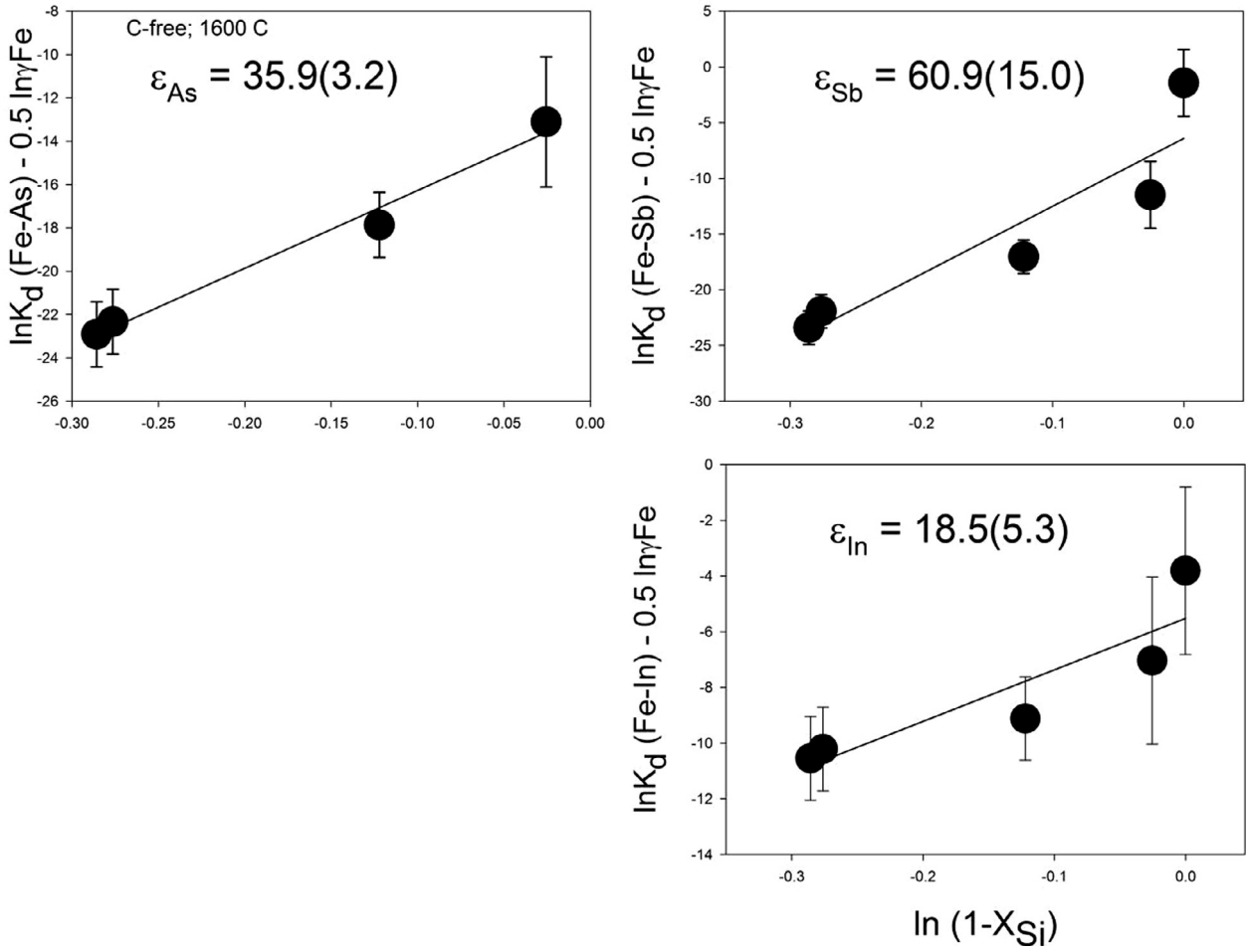

Fig. 6. Ln K_d(Fe–M)–(n/2–1) ln γ_{Fe}^{metal} vs. ln(1 − X_{Si}) for As, Sb, Ge, and In at 1600 °C in C-free experiments (MgO capsules). Solid lines are a linear fit to the data and the slope of each line is the ε_M^{Si} with associated error. Only one Ge data point is available in the C-free (MgO capsule) series and it is plotted in Fig. 4.

can be assessed with D(In) metal/silicate exhibiting only weak dependence on melt composition, whereas D(Ge) metal/silicate ($d = -0.26$), D(As) metal/silicate ($d = -0.24$), and D(Sb) metal/silicate ($d = -0.73$) all show a stronger dependence. Previous work has shown that highly charged cations can be more sensitive to silicate melt composition (Righter, 2003); Sb(3+) does in this study, but In(3+), Ge (2+), and As(3+) all show only a moderate effect, suggesting that not all highly charged cations have a strong dependence on melt composition.

5.3. Application to Earth

The origin of volatiles in Earth's primitive mantle has been ascribed to various sources, including indigenous (Halliday, 2013; Saal et al., 2013) or exogenous such as comets (Delsemme, 1997) or a late veneer (Albarède, 2009; Ballhaus et al., 2013). Exogenous sources may be required if indigenous processes cannot account for the observations. To place better constraints on the origin of the volatile siderophile element (VSE) abundances and the possible need for a late veneer or late accretion, we model the VSE content resulting from metal–silicate equilibrium in a terrestrial magma ocean environment and compare these to observations. Previous models of volatile siderophile element distributions have been based on incomplete datasets or a limited set of elements (Righter and Drake, 2000; Mann et al., 2009; Ballhaus et al., 2013). Our new data, combined with previously reported data for volatile siderophile elements, allows modelling to include the effects of a wider range of P, T, fO_2, and silicate melt composition, and the effects of S, C, and Si on the metal activity coefficients. Using these new regressions, we will re-evaluate indigenous and exogenous models based on several volatile siderophile elements.

Recent models of a terrestrial magma ocean predict that moderately siderophile element depletions in Earth's primitive upper mantle can be explained by metal–silicate equilibrium between metallic and silicate liquid at high PT conditions during Earth's accretion (~40 GPa, ~3400 K; e.g., Righter et al., 2008; Righter, 2011a; Siebert et al., 2011, 2012; Wade et al., 2012; Fischer et al., 2015). There is some debate about the specific PT conditions, and whether the oxygen fugacity in the mantle changed during

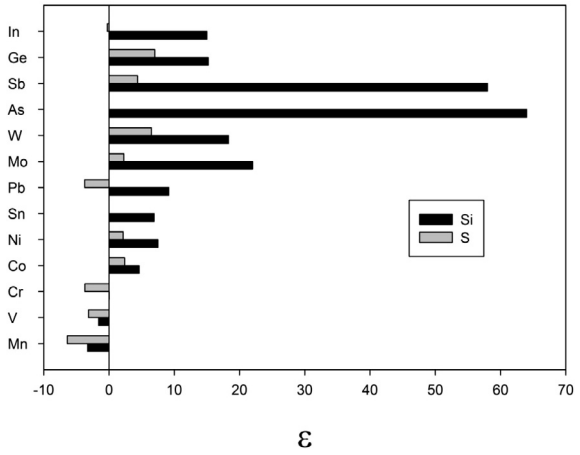

Fig. 7. Comparison of epsilon values for As, Sb, Ge, and In in Si-bearing Fe metallic liquid to those determined in previous studies for S-bearing metallic liquids (Wood et al., 2014). Also shown are values of epsilon parameters for other moderately and slightly siderophile elements from Tuff et al. (2011), Wood et al. (2014), and Steel Making Handbook (1988).

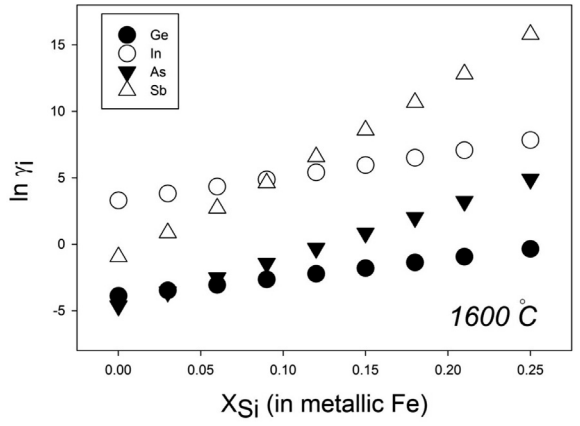

Fig. 8. $\ln\gamma$(M) for As, Sb, Ge and In vs. mole fraction of Si in the metallic Fe liquid, calculated at 1600 °C, showing the strong effect of dissolved Si on the activities of these metals. $\ln\gamma$(M) values are calculated using epsilon parameters derived here (as well as those in Wade and Wood (2005), Wade et al. (2012), and Wood et al. (2014)), and using the activity model of Ma (2001).

accretion or was relatively constant. Modelling suggests that fO_2 started low and eventually became higher during accretion (e.g., Wood et al., 2006; Rubie et al., 2011), whereas some recent calculations indicate that fO_2 may have decreased or changed only slightly during accretion (Siebert et al., 2013 and Righter and Ghiorso, 2012a,b, respectively). If the oxygen fugacity is changing during accretion, the composition of core forming metallic liquid will also change because reduced conditions will favor Si dissolution (Righter et al., 2016), whereas oxidized conditions will favor S or C (Jana and Walker, 1997b). These light elements will exert a strong effect on the activity coefficients of each trace metal as we have seen in this study and discussed above.

Due to this uncertainty in the fO_2 evolution of the growing Earth, we examine the evolution of the composition of the Earth's PUM during continuous accretion considering two scenarios: one with nearly constant fO_2 (IW-2) and one with increasing fO_2 (IW-4 to IW-2). Calculations have been carried out along the PT conditions of the liquidus for peridotite, according to Andrault et al. (2011). On this path, the Earth's mantle FeO content changes from $X_{FeO} = 0.01$–0.06. The core metallic liquid S, C, and Si composition is calculated according to the metal–silicate partitioning studies of Boujibar et al. (2014), Chi et al. (2014), and Siebert et al. (2013), respectively. Equilibration occurs instantaneously so that as the Earth grows there is constant re-equilibration between the core and mantle (e.g., Deguen et al., 2014; Kendall and Melosh, 2016). The equation used to calculate mantle concentrations is:

$$C^i_{LS} = \frac{C^i_{bulk}}{x[p + (1-p)D^i_{SS/LS}] + (1-x)[D^i_{LM/LS}]} \quad (9)$$

where x is the fraction of silicate, p is the fraction of molten silicate, C^i_{bulk} is the bulk concentration of siderophile element, C^i_{LS} the concentration of siderophile element in the liquid silicate, $D^i_{SS/LS}$ is the partition coefficient between solid silicate and liquid silicate, and $D^i_{LM/LS}$ (= D(M) here) is the partition coefficient between liquid metal and liquid silicate (Righter et al., 1997). For Earth calculations, $x = 0.68$, and $p = 0.6$; $D^i_{LM/LS}$ is calculated using Eq. (8) and the regression coefficients in Table S5, and $D^i_{SS/LS}$ is $<<1$ for As and Sb and ~ 1 for In and Ge (e.g., Suzuki and Akaogi, 1995; Adam and Green, 2006; Righter et al., 2009).

The bulk Earth values used in this modelling are based on CI chondrites (Newsom, 1995). Bulk Earth values for volatile elements are usually corrected for volatility according to volatility trends as defined by McDonough and Sun (1995) or Lodders (2003), for example. An alternative approach is to consider bond energies (e.g., Albarède et al., 2015); in general the agreement between the 50% condensation temperature and bond energy is good, indicating either approach yields a similar volatility correction. However, In is an exception: In concentration typically falls higher than the standard volatility trend, and is thus suspect. But the host phase for In is not well understood and thus there is great uncertainty in the correction for In. If one considers the bond energy of InS, and assumes that sulfide may be the host phase for In, the value of ~289 kJ per-mol (Cottrell, 1958) corresponds to 50% condensation temperature of 800 K and instead of 536 K as tabulated by Lodders (2003). If this higher value is adopted, the volatility correction for In is smaller. So, the most volatile element considered here – In – has been corrected by a factor of 4, resulting in a bulk Earth In content of 20 ppb (CI = 80 ppb). Germanium, As, and Sb all have similar volatilities (50% condensation temperatures of 900–1000 K) and have been corrected by a factor of 3, resulting in bulk Ge, As, and Sb contents of 11 ppb (CI = 32 ppb), 620 ppb (CI = 1860 ppb), and 47 ppb (CI = 140 ppb), respectively.

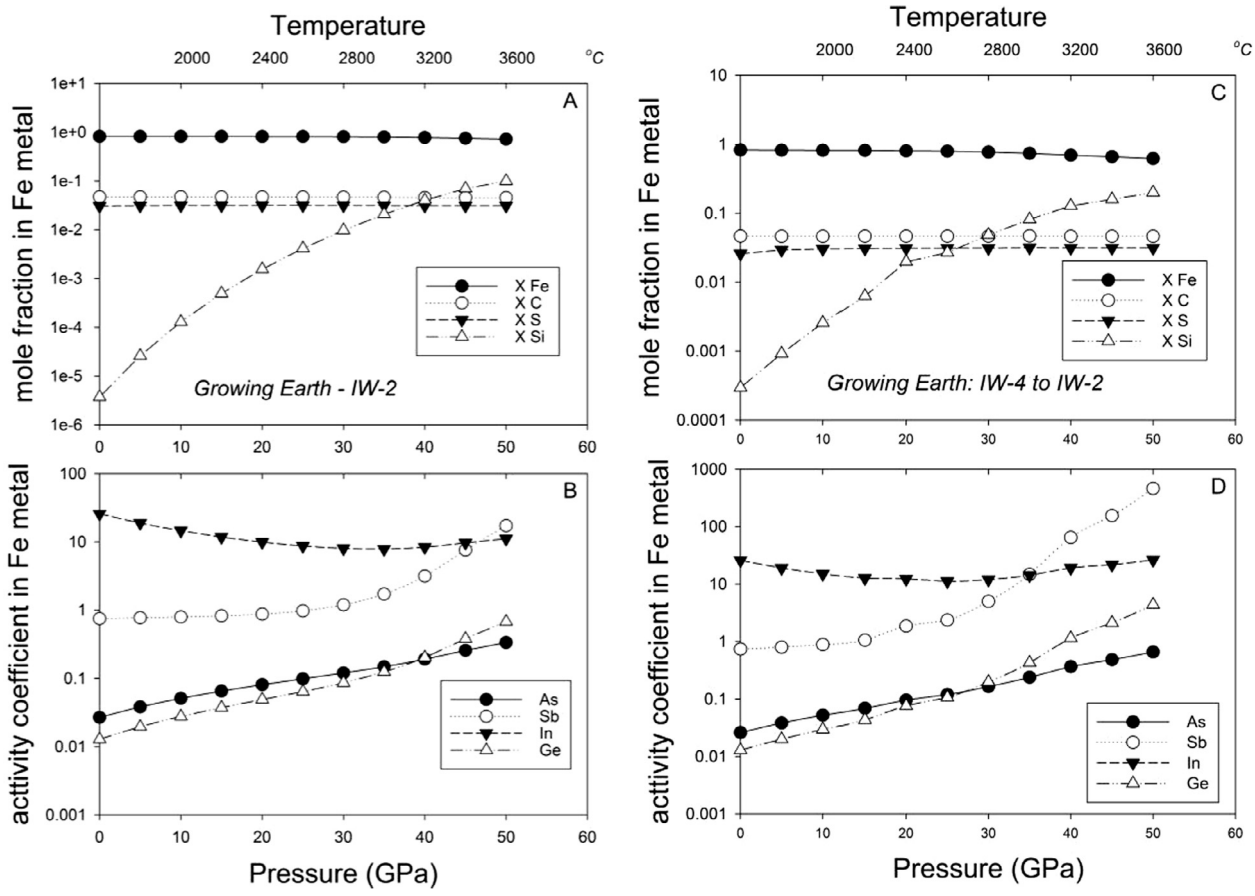

Fig. 9. (A) Comparison of Fe, S, C, and Si content of the core forming metallic Fe liquid as accretion proceeds for relatively constant fO_2 path (IW-2) during accretion. (B) Variation of activity coefficients for As, Sb, Ge, and In during the same accretion model as A, illustrating the large effect of changing Fe metallic liquid composition on the activity coefficients. (C) Comparison of Fe, S, C, and Si content of the core forming metallic Fe liquid for a model where accretion starts reduced (IW-4) and finishes more oxidized (IW-2). (D) Variation of activity coefficients for As, Sb, Ge, and In during the same accretion model as C, illustrating the large effect of changing Fe metallic liquid composition on the activity coefficients. *PT* curve for calculations is along peridotite liquidus of Andrault et al. (2011). The final core composition for this second model is 10.2% Si, 2% S, and 1.1% C (or $X_{Si} = 0.18$, $X_S = 0.03$, and $X_C = 0.04$.

As the Earth grows, the S, C and Si content of the core metal changes - because D(metal/silicate) for S and C remain very high during this interval, the S and C content of the core do not change much because essentially all S and C available in the chondritic building blocks partitions into the core. Si, on the other hand, increases substantially in the core as the Earth grows (Fig. 9A, C). The final core composition is 10.2% Si, 2% S, and 1.1% C (or $X_{Si} = 0.18$, $X_S = 0.03$, and $X_C = 0.04$). Calculated concentrations of As, Sb, Ge, and In in the Earth's magma ocean during accretion and differentiation are shown in Fig. 10 compared to the values of each measured in the bulk silicate Earth (BSE). During the accretion process, the mantle In contents stay high, but are continuously lowered due to pressure effects. The In content of the PUM can be achieved at pressures higher than ~20 GPa. Arsenic and Sb, on the other hand, stay very low during the early part of accretion (Fig. 10), but can achieve the PUM concentration levels near the end of accretion at pressures >30–40 GPa. This is achieved at a slightly lower pressure for the "reduced to oxidized" scenario, due to the effect of greater Si concentration in the core-forming metal. Germanium content of the PUM is also achieved at high pressure >35 GPa, in either scenario, with the "reduced to oxidized" scenario achieving these concentrations at a slightly lower pressure for the same reason as discussed above. These calculations suggest that the volatile siderophile elements can be explained by a rather simple scenario of continuous accretion coupled with high PT metal–silicate equilibrium that establishes the siderophile element content of Earth's PUM near the end of accretion. There is some advantage to examining elemental ratios as well (Mann et al., 2009), and consideration of In/Ge ratios illustrate that although this ratio is far from mantle values at the low pressure conditions early in the accretion process, it becomes very close to mantle values at the higher pressures of 35–45 GPa achieved in the magma ocean near the end of accretion (Fig. 11). These results are not strongly dependent upon the fO_2 during accretion, although the "reduced to oxidized" scenario modelled here allows attainment of PUM levels of In, As and Ge at slightly lower pressures compared to the "constant fO_2" scenario.

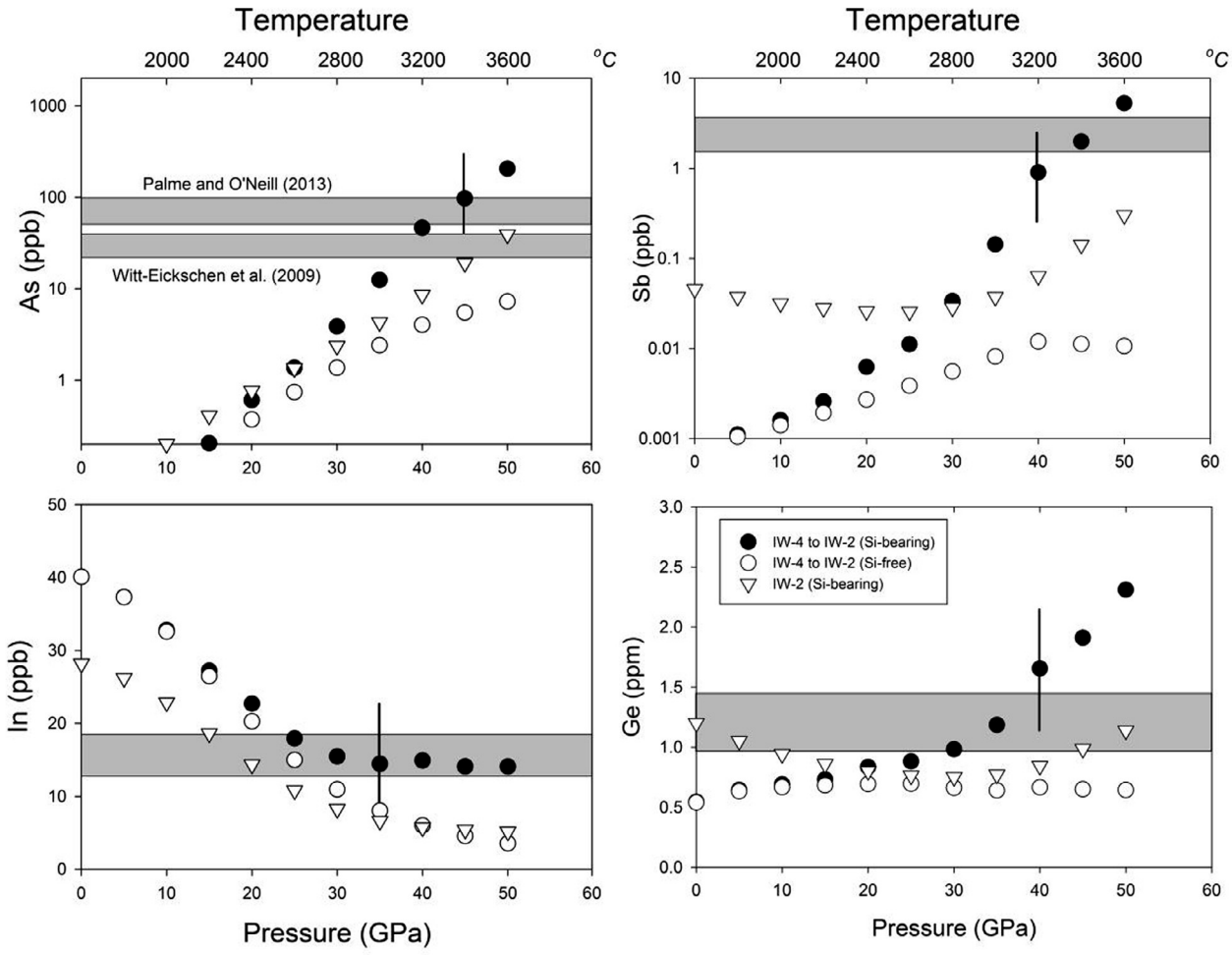

Fig. 10. Evolution of Earth's mantle volatile siderophile elements as accretion proceeds for three different scenarios: accretion with fO_2 nearly constant (triangles), and fO_2 increasing (closed circles), and fO_2 increasing but calculated for Si-free metallic liquids (open circles) to illustrate the specific effect of Si. PT curve for calculations is along peridotite liquidus of Andrault et al. (2011). Horizontal bands represent terrestrial primitive upper mantle values (and associated uncertainty) for each element, from Table S4. Error bars on theh calculated values include 1 sigma uncertainty in regressions presented in Table S5, as well as uncertainty in the volatility correction for the bulk Earth concentrations. The partition coefficients calculated at 45 GPa (near the base of the magma ocean) are D(Sb) = 50, D(As)) = 13, D(Ge)) = 34, and D(In)) = 2.9.

This is not a single stage core formation model (e.g., Walter and Cottrell, 2013), nor does it require late stage addition of chondritic materials (e.g., Chou, 1978; Rose-Weston et al., 2009; Ballhaus et al., 2013). Our results are similar to the results of Mann et al. (2009) based on In and additional weakly siderophile and volatile elements Ta, Nb, V, Cr, Mn, Ga and Zn. Equilibrium was attained during each accreting step so that the last equilibration event involves equilibration between the core metal and a mantle that has previously equilibrated with FeNi metallic liquid at high pressure and the chemical difference is minor. This equilibration scenario is consistent with, for example, recent Mo isotopic measurements indicating that Mo in Earth's PUM equilibrated with the core (Greber et al., 2015), as well as physical modelling suggesting equilibrium between metal and silicate is extensive (Deguen et al., 2014; Kendall and Melosh, 2016).

6. SUMMARY AND CONCLUSIONS

Our new results demonstrate that Si has a large effect on the metal–silicate partitioning of As, Sb, Ge, and In. Si has the greatest effect on Sb, followed by As, Ge, and In. Increasing temperature decreases the K_d (Fe–M) and D (metal/silicate) for all of the elements; temperatures higher than 2000 °C are needed to explain equilibrium between core and mantle. It is clear that the effect of Si and temperature need to be quantified in order to apply metal–silicate partition coefficients to Earth, Moon, or any differentiated body. Based on a combination of our new data and previously published data, the concentrations of these elements in the primitive mantle can be explained by high pressure and temperature equilibration between the core and silicate melt during accretion, either at fixed fO_2 or variable fO_2 from early reduced to later oxidized. This supports the

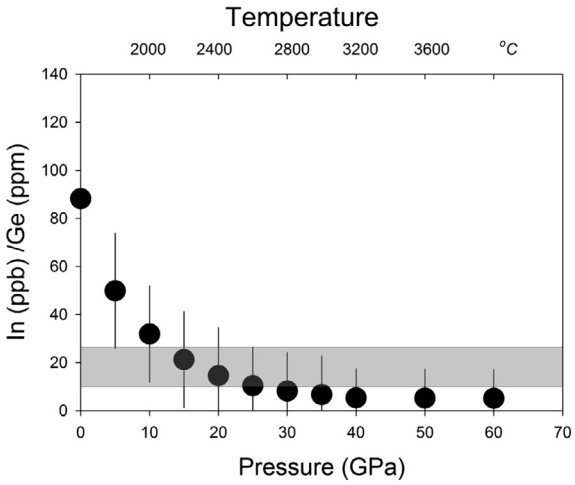

Fig. 11. In/Ge during the accretion model with variable fO_2 (early reduced and later oxidized). Horizontal colored bands show the primitive mantle values from Table S4. Partitioning values used for Ge and In are calculated using regression parameters from Table S5. PT curve for calculations is the same as in Figs. 9 and 10.

hypothesis that volatile elements were present during Earth's accretion and core formation (e.g., Halliday, 2013), and in general, that volatiles have an indigenous rather than exogenous (post accretion) origin.

The concentrations of these four elements in Earth's primitive upper mantle can be explained by a combination of core formation and volatility, but we can't rule out the possibility that the Earth had non-chondritic building blocks, as suggested by Drake and Righter (2002), Dauphas et al. (2014) or Wang et al. (2016). Future work may focus on the effect of pressure on siderophile element valence; much of our understanding of valences is based on detailed work at low pressures. The valence of some elements such as V, Cr, Mo, and W is not significantly affected by pressure (e.g., Righter et al., 2011b, 2016; Wade et al., 2013), whereas other elements such as Ta and Nb could be significantly affected (Cartier et al., 2015). Because every element may have unique behavior, there may be additional studies needed of siderophile element valences in high pressure silicate melts. In addition, calculations of mantle concentrations of most siderophile elements are based on low pressure experimental data and require extrapolation to the higher pressures indicated by the modelling. Although the extrapolation procedures have been shown to be robust in many cases (e.g., Ni – Righter, 2011b), there is nonetheless a dearth of data at higher pressures relevant to deep magma oceans and this should be addressed in future studies as well.

ACKNOWLEDGEMENTS

This work was supported by RTOPs from the NASA Cosmochemistry and LASER programs to KR. KN was supported by an LPI summer internship. We thank A. Peslier and K. Ross for their assistance with the electron microprobe at JSC, C.-T. Lee and P. Luffi for access to and assistance with the LA-ICP-MS at Rice University, and Yongjun Gao for assistance with the Q-ICP-MS at Univ. of Houston. We thank R. Dasgupta for loan of the carbon standard for microprobe analysis. Discussions with M. Humayun, F. Moynier, M. Rutherford, D. Kring, and colleagues with the LPI-JSC NLSI team helped to formulate the ideas and issues discussed in this paper. Early versions of the manuscript benefitted greatly from comments and suggestions of M. Norman, C. Ballhaus, and E. Cottrell. The two anonymous journal reviews and comments of the AE W. van Westrenen also improved the clarity of the presentation.

APPENDIX A. SUPPLEMENTARY DATA

Supplementary data associated with this article can be found, in the online version, at http://dx.doi.org/10.1016/j.gca.2016.10.045.

REFERENCES

Adam J. and Green T. (2006) Trace element partitioning between mica-and amphibole-bearing garnet lherzolite and hydrous basanitic melt: 1. Experimental results and the investigation of controls on partitioning behaviour. *Contrib. Miner. Petrol.* **152**, 1–17.

Agrinier A. and Lee C.-T. (2007) Quantifying trace element disequilibria in mantle xenoliths and abyssal peridotite. *Earth Planetary Sci. Lett.* **257**, 290–298.

Albarède F. (2009) Volatile accretion history of the terrestrial planets and dynamic implications. *Nature* **461**, 1227–1233.

Albarède F., Albalat E. and Lee C. T. A. (2015) An intrinsic volatility scale relevant to the Earth and Moon and the status of water in the Moon. *Meteorit. Planet. Sci.* **50**, 568–577.

Andrault D., Bolfan-Casanova N., Lo Nigro G., Bouhifd M. A., Garbarino G. and Mezouar M. (2011) Solidus and liquidus profiles of chondritic mantle: Implication for melting of the Earth across its history. *Earth Planet. Sci. Lett.* **304**, 251–259.

Ballhaus C., Laurenz V., Münker C., Fonseca R. O. C., Albarède F., Rohrbach A., Lagos M., Schmidt M. W., Jochum K.-P., Stoll B., Weis U. and Helmy H. M. (2013) The U/Pb ratio of the Earth's mantle—A signature of late volatile addition. *Earth Planet. Sci. Lett.* **362**, 237–245.

Berthet S., Malavergne V. and Righter K. (2009) Evolution of Indarch (EH4 chondrite) at 1 GPa and high temperature: implications for early planetary differentiation processes. *Geochim. Cosmochim. Acta* **73**, 6402–6420.

Blanchard I., Badro J., Siebert J. and Ryerson F. J. (2015) Composition of the core from gallium metal–silicate partitioning experiments. *Earth Planet. Sci. Lett.* **427**, 191–201.

Boujibar A., Andrault D., Bouhifd M. A., Bolfan-Casanova N., Devidal J. L. and Trcera N. (2014) Metal–silicate partitioning of sulphur, new experimental and thermodynamic constraints on planetary accretion. *Earth Planet. Sci. Lett.* **391**, 42–54.

Campbell A. J., Danielson L., Righter K., Seagle C. T., Wang Y. and Prakapenka V. B. (2009) High pressure effects on the iron–iron oxide and nickel–nickel oxide oxygen fugacity buffers. *Earth Planet. Sci. Lett.* **286**, 556–564.

Capobianco C. J., Drake M. J. and DeAro J. (1999) Siderophile geochemistry of Ga, Ge, and Sn: cationic oxidation states in silicate melts and the effect of composition in iron–nickel alloys. *Geochim. Cosmochim. Acta* **63**, 2667–2677.

Cartier C., Hammouda T., Boyet M., Mathon O., Testemale D. and Moine B. N. (2015) Evidence for Nb^{2+} and Ta^{3+} in silicate melts under highly reducing conditions: a XANES study. *Am. Mineral.* **100**, 2152–2158.

Chabot N. L., Campbell A. J., Jones J. H., Humayun M. and Agee C. B. (2003) An experimental test of Henry's Law in solid

metal-liquid metal systems with implications for iron meteorites. *Meteorit. Planet. Sci.* **38**, 181–196.

Chi H., Dasgupta R., Duncan M. S. and Shimizu N. (2014) Partitioning of carbon between Fe-rich alloy melt and silicate melt in a magma ocean – implications for the abundance and origin of volatiles in Earth, Mars, and the Moon. *Geochim. Cosmochim. Acta* **139**, 447–471.

Chou C. L. (1978) Fractionation of siderophile elements in the Earth's upper mantle. *Proc. Lunar Planet. Sci. Conf. 9th.* pp. 219–230.

Cottrell T. L. (1958) *The Strengths of Chemical Bonds*, second ed. Butterworth, London.

Cottrell E., Walter M. J. and Walker D. (2009) Metal–silicate partitioning of tungsten at high pressure and temperature: implications for equilibrium core formation in Earth. *Earth Planet. Sci. Lett.* **281**, 275–287.

Cottrell E., Walter M. J. and Walker D. (2010) Erratum to "metal–silicate partitioning of tungsten at high pressure and temperature: Implications for equilibrium core formation in Earth" [Earth and Planetary Science Letters 281 (2009) 275–287]. *Earth Planet. Sci. Lett.* **289**, 631–634.

Dasgupta R., Chi H., Shimizu N., Buono A. S. and Walker D. (2013) Carbon solution and partitioning between metallic and silicate melts in a shallow magma ocean: implications for the origin and distribution of terrestrial carbon. *Geochim. Cosmochim. Acta* **102**, 191–212.

Dauphas N., Chen J. H., Zhang J., Papanastassiou D. A., Davis A. M. and Travaglio C. (2014) Calcium-48 isotopic anomalies in bulk chondrites and achondrites: evidence for a uniform isotopic reservoir in the inner protoplanetary disk. *Earth Planet. Sci. Lett.* **407**, 96–108.

Deguen R., Landeau M. and Olson P. (2014) Turbulent metal–silicate mixing, fragmentation, and equilibration in magma oceans. *Earth Planet. Sci. Lett.* **391**, 274–287.

Delsemme A. (1997) The origin of the atmosphere and of the oceans. In *Comets and the Origin and Evolution of Life*. Springer, New York, pp. 29–67.

Drake M. J. and Righter K. (2002) Determining the composition of the Earth. *Nature* **416**, 39–44.

Fischer R. A., Nakajima Y., Campbell A. J., Frost D. J., Harries D., Langenhorst F. and Rubie D. C. (2015) High pressure metal–silicate partitioning of Ni Co, V, Cr, Si, and O. *Geochim. Cosmochim. Acta* **167**, 177–194.

Gessmann C. K., Rubie D. C. and McCammon C. A. (1999) Oxygen fugacity dependence of Ni Co, Mn, Cr, V, and Si partitioning between liquid metal and magnesiowüstite at 9–18 GPa and 2200 °C. *Geochim. Cosmochim. Acta* **63**, 1853–1863.

Greber N. D., Puchtel I. S., Nägler T. F. and Mezger K. (2015) Komatiites constrain molybdenum isotope composition of the Earth's mantle. *Earth Planet. Sci. Lett.* **421**, 129–138.

Halliday A. N. (2013) The origins of volatiles in the terrestrial planets. *Geochim. Cosmochim. Acta* **105**, 146–171.

Hillgren V. J., Drake M. J. and Rubie D. C. (1996) High pressure and high temperature metal–silicate partitioning of siderophile elements: the importance of silicate liquid composition. *Geochim. Cosmochim. Acta* **60**, 2257–2263.

Holzheid A., Palme H. and Chakraborty S. (1997) The activities of NiO, CoO and FeO in silicate melts. *Chem. Geol.* **139**, 21–38.

Jana D. and Walker D. (1997a) The influence of silicate melt composition on distribution of siderophile elements among metal and silicate liquids. *Earth Planet. Sci. Lett.* **150**, 463–472.

Jana D. and Walker D. (1997b) The influence of sulfur on partitioning of siderophile elements. *Geochim. Cosmochim. Acta* **61**, 5255–5277.

Kegler P. and Holzheid A. (2011) Determination of the formal Ge-oxide species in silicate melts at oxygen fugacities applicable to terrestrial core formation scenarios. *Eur. J. Mineral.* **23**, 369–378.

Kegler P., Holzheid A., Frost D. J., Rubie D. C., Dohmen R. and Palme H. (2008) New Ni and Co metal–silicate partitioning data and their relevance for an early terrestrial magma ocean. *Earth Planet. Sci. Lett.* **268**, 28–40.

Kendall J. and Melosh H. J. (2016) Differentiated planetesimal impacts into a terrestrial magma ocean: fate of the iron core. *Earth Planet. Sci. Lett.* **448**, 24–33.

Lewis R. D., Lofgren G. E., Franzen H. F. and Windom K. E. (1993) The effect of Na vapor on the Na content of chondrules. *Meteoritics* **28**, 622–628.

Li J. and Agee C. B. (2001) The effect of pressure, temperature, oxygen fugacity and composition on partitioning of nickel and cobalt between liquid Fe–Ni–S alloy and liquid silicate: implications for the earth's core formation. *Geochim. Cosmochim. Acta* **65**, 1821–1832.

Lodders K. (2003) Solar system abundances and condensation temperatures of the elements. *Astrophys. J.* **591**, 1220–1247.

Lupis C. H. (1983) *Chemical thermodynamics of materials*. Elsevier Science Publishing Co., Inc, UK, p. 581.

Ma Z. (2001) Thermodynamic description for concentrated metallic solutions using interaction parameters. *Metall. Mater. Trans. B* **32**, 87–103.

Mann U., Frost D. J. and Rubie D. C. (2009) Evidence for high-pressure core-mantle differentiation from the metal–silicate partitioning of lithophile and weakly siderophile elements. *Geochim. Cosmochim. Acta* **73**, 7360–7386.

McDonough W. F. and Sun S. (1995) The composition of the Earth. *Chem. Geol.* **120**, 223–253.

Mills K. C. (1993) The influence of structure on the physico-chemical properties of slags. *ISIJ Int.* **33**, 148–155.

Morard G. and Katsura T. (2010) Pressure–temperature cartography of Fe–S–Si immiscible system. *Geochim. Cosmochim. Acta* **74**, 3659–3667.

Musselwhite D. S., Dalton H. A., Kiefer W. S. and Treiman A. H. (2006) Experimental petrology of the basaltic shergottite Yamato-980459: implications for the thermal structure of the Martian mantle. *Meteorit. Planet. Sci.* **41**, 1271–1290.

Mysen B. O. (1991) Volatiles in magmatic liquids. In *Physical Chemistry of Magma* (eds. L. L. Perchuk and I. Kushiro). Cambridge University Press, New York, pp. 435–476 (Ch. 16).

Newsom H. E. (1995) *Composition of the Solar System, Planets, Meteorites, and Major Terrestrial Reservoirs, AGU Reference Shelf 1, 159–189*. Cambridge University Press.

O'Neill H. and St C. (1992) Siderophile elements and the Earth's formation. Technical comment. *Science* **257**, 1282–1284.

Palme H. and O'Neill H. S. C. (2014) *Cosmochemical estimates of mantle composition. Treatise on Geochemistry*, 2 (2nd ed.), pp. 1–39.

Righter K. (2003) Metal–silicate partitioning of siderophile elements and core formation in the early Earth and terrestrial planets. *Ann. Rev. Earth Planet. Sci.* **31**, 135–174.

Righter K. (2007) High pressure, temperature experimental constraints on Volatile, siderophile element depletions (Cd, In) in mantles. 70th Annual Meteoritical Society Meeting, held in August 13–17, Arizona. *Meteorit. Planet. Sci. Suppl.* **42**, 5195.

Righter K. (2011a) Prediction of metal–silicate partition coefficients for siderophile elements: an update and assessment of PT conditions for metal–silicate equilibrium during accretion of the Earth. *Earth Planet. Sci. Lett.* **304**, 158–167.

Righter K. (2011b) Reply to the Comment by Palme et al. on "Prediction of metal–silicate partition coefficients for siderophile elements: An update and assessment of PT conditions

for metal–silicate equilibrium during accretion of the Earth". *Earth Planet. Sci. Lett.* **312**, 519–521.

Righter K. and Drake M. J. (1999) Effect of water on metal–silicate partitioning of siderophile elements: a high pressure and temperature terrestrial magma ocean and core formation. *Earth Planet. Sci. Lett.* **171**, 383–399.

Righter K. and Drake M. J. (2000) Metal–silicate equilibrium in the early Earth: new constraints from volatile moderately siderophile elements Ga, Sn, Cu and P. *Geochim. Cosmochim. Acta* **64**, 3581–3597.

Righter K. and Ghiorso M. S. (2012a) Redox systematics of a magma ocean with variable pressure-temperature gradients and composition. *Proc. Natl. Acad. Sci.* **109**, 11955–11960.

Righter K. and Ghiorso M. S. (2012b) Correction for Righter and Ghiorso, redox systematics of a magma ocean with variable pressure-temperature gradients and composition. *Proc. Natl. Acad. Sci.* **109**, 16749–16750.

Righter K., Drake M. J. and Yaxley G. (1997) Prediction of siderophile element metal–silicate partition coefficients to 20 GPa and 2800 °C: the effects of pressure, temperature, oxygen fugacity, and silicate and metallic melt compositions. *Phys. Earth Planet. Inter.* **100**, 115–134.

Righter K., Humayun M. and Danielson L. R. (2008) High pressure and temperature partitioning of palladium during core formation. *Nat. Geosci.* **1**, 321–323.

Righter K., Humayun M., Campbell A. J., Danielson L. R., Hill D. and Drake M. J. (2009) Experimental studies of metal–silicate partitioning of Sb: implications for the terrestrial and lunar mantles. *Geochim. Cosmochim. Acta* **73**, 1487–1504.

Righter K., Pando K., Danielson L. R. and Lee C.-T. (2010) Partitioning of Mo, P and other siderophile elements (Cu, Ga, Sn, Ni Co, Cr, Mn, V, W) between metal and silicate melt as a function of temperature and melt composition. *Earth Planet. Sci. Lett.* **291**, 1–9.

Righter K., King C., Danielson L. R., Pando K. and Lee C. T. (2011a) Experimental determination of the metal/silicate partition coefficient of Germanium: implications for core and mantle differentiation. *Earth Planet. Sci. Lett.* **304**, 379–388.

Righter K., Sutton S., Danielson L., Pando K., Schmidt G., Yang H., Berthet S., Newville M., Choi Y., Downs R. T. and Malavergne V. (2011b) The effect of fO_2 on the partitioning and valence of V and Cr in garnet/melt pairs and the relation to terrestrial mantle V and Cr content. *Am. Mineral.* **96**, 1278–1290.

Righter K., Danielson L. R., Pando K. M., Shofner G. A., Sutton S. R., Newville M. and Lee C. T. (2016) Valence and metal/silicate partitioning of Mo: implications for conditions of Earth accretion and core formation. *Earth Planet. Sci. Lett.* **437**, 89–100.

Rose-Weston L., Brenan J. M., Fei Y., Secco R. A. and Frost D. J. (2009) Effect of pressure, temperature, and oxygen fugacity on the metal–silicate partitioning of Te, Se, and S: implications for earth differentiation. *Geochim. Cosmochim. Acta* **73**, 4598–4615.

Rubie D. C., Frost D. J., Mann U., Asahara Y., Nimmo N., Tsuno K., Kegler P., Holzheid A. and Palme H. (2011) Heterogeneous accretion, composition and core–mantle differentiation of the Earth. *Earth Planet. Sci. Lett.* **301**, 31–42.

Saal A. E., Hauri E. H., Van Orman J. A. and Rutherford M. J. (2013) Hydrogen isotopes in lunar volcanic glasses and melt inclusions reveal a carbonaceous chondrite heritage. *Science* **340**, 1317–1320.

Siebert J., Badro J., Antonangeli D. and Ryerson F. J. (2012) Metal–silicate partitioning of Ni and Co in a deep magma ocean. *Earth Planet. Sci. Lett.* **321–322**, 189–197.

Siebert J., Badro J., Antonangeli D. and Ryerson F. J. (2013) Terrestrial accretion under oxidizing conditions. *Science* **339**, 1194–1197.

Siebert J., Corgne A. and Ryerson F. J. (2011) Systematics of metal–silicate partitioning for many siderophile elements applied to Earth's core formation. *Geochim. Cosmochim. Acta* **75**, 1451–1489.

Steelmaking J. (1988) *Steelmaking Data Sourcebook*. Gordon and Breach Science Publishers, Montreux.

Suzuki T. and Akaogi M. (1995) Element partitioning between olivine and silicate melt under high pressure. *Phys. Chem. Miner.* **22**, 411–418.

Tuff J., Wood B. J. and Wade J. (2011) The effect of Si on metal–silicate partitioning of siderophile elements and implications for the conditions of core formation. *Geochim. Cosmochim. Acta* **75**, 673–690.

van Achterbergh E., Ryan C.G., and Griffin W. L. (1999) GLITTER: on-line interactive data reduction for the laser ablation ICP-MS microprobe. In *9th Annual V.M. Goldschmidt Conference*, pp 305–306.

Wade J. and Wood B. J. (2005) Core formation and the oxidation state of the Earth. *Earth Planet. Sci. Lett.* **236**, 78–95.

Wade J., Wood B. J. and Tuff J. (2012) Metal–silicate partitioning of Mo and W at high pressures and temperatures: evidence for late accretion of sulphur to the Earth. *Geochim. Cosmochim. Acta* **85**, 58–74.

Wade J., Wood B. J. and Norris C. A. (2013) The oxidation state of tungsten in silicate melt at high pressures and temperatures. *Chem. Geol.* **335**, 189–193.

Walker D., Norby L. and Jones J. H. (1993) Superheating effects on metal–silicate partitioning of siderophile elements. *Science* **262**, 1858–1861.

Walter M. J. and Cottrell E. (2013) Assessing uncertainty in geochemical models for core formation in Earth. *Earth Planet. Sci. Lett.* **365**, 165–176.

Walter M. J. and Thibault Y. (1995) Partitioning of tungsten and molybdenum between metallic liquid and silicate melt. *Science* **270**, 1186–1189.

Wang Z., Laurenz V., Petitgirard S. and Becker H. (2016) Earth's moderately volatile element composition may not be chondritic: Evidence from In, Cd, and Zn. *Earth Planet. Sci. Lett.* **435**, 136–146.

Wasson J. T. (1985) *Meteorites: Their Record of Early Solar-System History*. W. H. Freeman and Co., New York, p. 274.

Witt-Eickschen G., Palme H., O'Neill H. St. and Allen C. C. M. (2009) The geochemistry of the volatile trace elements As, Cd, Ga, In and Sn in the Earth's mantle: new evidence from in situ analyses of mantle xenoliths. *Geochim. Cosmochim. Acta* **73**, 1755–1778.

Wood B. J., Walter M. J. and Wade J. (2006) Accretion of the Earth and segregation of its core. *Nature* **441**, 825–833.

Wood B. J., Kiseeva E. S. and Mirolo F. J. (2014) Accretion and core formation: the effects of sulfur on metal–silicate partition coefficients. *Geochim. Cosmochim. Acta* **145**, 248–267.

Yi W., Halliday A. N., Alt J. C., Lee D.-C., Rehkämper M., Garcia M. O. and Su Y. (2000) Cadmium, indium, tin, tellurium, and sulfur in oceanic basalts: Implications for chalcophile element fractionation in the Earth. *J. Geophys. Res.* **105**, 18927–18948.

Ziegler K., Young E. D., Schauble E. A. and Wasson J. T. (2010) Metal–silicate silicon isotope fractionation in enstatite meteorites and constraints on Earth's core formation. *Earth Planet. Sci. Lett.* **295**, 487–496.

Associate editor: Wim van Westrenen